

AD-A213 246

DTIC FILE COPY

20030205212

(2)

AD _____

FORMULATION OF TOPICAL PROTECTANTS/DECONTAMINANTS

Annual Report

DTIC
ELECTE
OCT 11 1989
S D & D

John L. Lach
Dale Eric Wurster
Lloyd E. Matheson, Jr.

March 14, 1987

Supported by

U.S. Army Medical Research and Development Command
Fort Detrick, Frederick, Maryland 21701-5012

Contract No. DAMD17-86-C-6127

College of Pharmacy
University of Iowa
Iowa City, IA 52242

Approved for public release; distribution unlimited

The findings in this report are not to be construed as an Official
Department of the Army position unless so designated by other
authorized documents.

89 10 1100E

REPORT DOCUMENTATION PAGE

Form Approved
OMB No 0704-0188

1a. REPORT SECURITY CLASSIFICATION Unclassified			1b. RESTRICTIVE MARKINGS		
2a. SECURITY CLASSIFICATION AUTHORITY			3. DISTRIBUTION/AVAILABILITY OF REPORT Approved for public release; distribution unlimited		
2b. DECLASSIFICATION/DOWNGRADING SCHEDULE			5. MONITORING ORGANIZATION REPORT NUMBER(S)		
4. PERFORMING ORGANIZATION REPORT NUMBER(S)			7a. NAME OF MONITORING ORGANIZATION		
6a. NAME OF PERFORMING ORGANIZATION University of Iowa College of Pharmacy		6b. OFFICE SYMBOL (if applicable)	7b. ADDRESS (City, State, and ZIP Code)		
6c. ADDRESS (City, State, and ZIP Code) Iowa City, IA 52242		9. PROCUREMENT INSTRUMENT IDENTIFICATION NUMBER Contract No. DAMD17-86-C-6127			
8a. NAME OF FUNDING/SPONSORING ORGANIZATION U.S. Army Medical Research & Development Command		8b. OFFICE SYMBOL (if applicable)	10. SOURCE OF FUNDING NUMBERS		
8c. ADDRESS (City, State, and ZIP Code) Fort Detrick, Frederick, Maryland 21701-5012		PROGRAM ELEMENT NO 63764A	PROJECT NO. 3764D995	TASK NO. BA	WORK UNIT ACCESSION NO 014
11. TITLE (Include Security Classification) Formulation of Topical Protectants/Decontaminants					
12. PERSONAL AUTHOR(S) John L. Lach, Dale Eric Wurster, Lloyd E. Matheson, Jr.					
13a. TYPE OF REPORT Annual Report		13b. TIME COVERED FROM 2/15/86 TO 2/14/87		14. DATE OF REPORT (Year, Month, Day) 1987 March 14	
				15. PAGE COUNT 35	
16. SUPPLEMENTARY NOTATION					
17. COSATI CODES			18. SUBJECT TERMS (Continue on reverse if necessary and identify by block number)		
FIELD	GROUP	SUB-GROUP	Fourier Transform Infrared Spectrophotometry, o-Iodosobenzoic Acid, Protective Barriers, Skin Decontamination		
			RAV		
19. ABSTRACT (Continue on reverse if necessary and identify by block number)					
<p>A technique employing Fourier transformation infrared (FTIR) spectrophotometry and the circle cell attachment was found to be useful for quantitating the amount of water solubilized in heptane by reverse micelles of dioctyl sodium sulfosuccinate. Use of FTIR spectrophotometry and the diffuse reflectance attachment to evaluate surface complexation reactions resulting from compression processes was less successful.</p> <p>Work was initiated on the catalysis of diisopropyl fluorophosphate (DFP) decomposition by o-Iodosobenzoic acid. This catalysis is insignificant in aqueous media unless a cationic surfactant is included at a concentration in excess of its critical micelle concentration. Although a substantial increase in DFP decomposition rate can be achieved, use of this system in the formulation of topical protectants will require that the problem of dermal irritation be solved.</p>					
20. DISTRIBUTION/AVAILABILITY OF ABSTRACT <input type="checkbox"/> UNCLASSIFIED/UNLIMITED <input type="checkbox"/> SAME AS RPT <input type="checkbox"/> DTIC USERS			21. ABSTRACT SECURITY CLASSIFICATION Unclassified		
22a. NAME OF RESPONSIBLE INDIVIDUAL Mrs. Virginia Miller			22b. TELEPHONE (Include Area Code) 301:663-7325		22c. OFFICE SYMBOL SGRD-RMI-S

AD _____

FORMULATION OF TOPICAL PROTECTANTS/DECONTAMINANTS

Annual Report

John L. Lach
Dale Eric Wurster
Lloyd E. Matheson, Jr.

March 14, 1987

Supported by

U.S. Army Medical Research and Development Command
Fort Detrick, Frederick, Maryland 21701-5012

Contract No. DAMD17-86-C-6127

College of Pharmacy
University of Iowa
Iowa City, IA 52242

Approved for public release; distribution unlimited

The findings in this report are not to be construed as an Official
Department of the Army position unless so designated by other
authorized documents.

Accession For	
NTIS CRA&I	<input checked="checked" type="checkbox"/>
DTIC TAB	<input type="checkbox"/>
Unannounced	<input type="checkbox"/>
Justification	
By	
Distribution/	
Availability Codes	
Dist	Avail and/or Special
A-1	

Summary

A technique employing Fourier transform infrared (FTIR) spectrophotometry and the circle cell attachment was found to be useful for quantitating the amount of water solubilized in heptane by reverse micelles of dioctyl sodium sulfosuccinate. Use of FTIR spectrophotometry and the diffuse reflectance attachment to evaluate surface complexation reactions resulting from compression processes was less successful.

Work was initiated on the catalysis of diisopropyl fluorophosphate (DFP) decomposition by o-iodosobenzoic acid. This catalysis is insignificant in aqueous media unless a cationic surfactant is included at a concentration in excess of its critical micelle concentration. Although a substantial increase in DFP decomposition rate can be achieved, use of this system in the formulation of topical protectants will require that the problem of dermal irritation be solved.

FOREWORD

In conducting research using animals, the investigator(s) adhered to the "Guide for the Care and Use of Laboratory Animals," prepared by the Committee on Care and Use of Laboratory Animals of the Institute of Laboratory Animal Resources, National Research Council (NIH Publication No. 86-23, Revised 1985).

Citations of commercial organizations and trade names in this report do not constitute an official Department of the Army endorsement or approval of the products or services of these organizations.

Table of Contents

<u>Subject</u>	<u>Page</u>
Summary	3
Foreword	5
List of Figures	9
List of Tables	11
Analysis by Fourier Transform Infrared Spectrophotometry	13
Introduction	13
Experimental Methods	15
Results and Discussion	16
o-Iodosobenzoic Acid Catalysis	21
Introduction	21
Experimental Methods	23
Results and Discussion	23
Conclusions	35
References	37
Distribution List	41

List of Figures

<u>Figure</u>		<u>Page</u>
1	Diffuse Reflectance FTIR Spectra of PVP/APAP Mixtures (3:1 by Weight) at Higher Compression Pressures.	17
2	Diffuse Reflectance FTIR Spectra of PVP/APAP Mixtures Compressed, Uncompressed, With and Without Mathematical Spectra Addition.	18
3	Calibration Plot for Water Solubilized in Heptane by Aerosol OT (Correlation Coefficient=0.9995).	20
4	Reaction Scheme for IBA.	22
5	Calibration Plot for the Fluoride Ion Electrode (Correlation Coefficient=0.9997).	24
6	Plot of Ln (Concentration) vs. Time for 0.0010 M DFP in a Solution of 0.00010 M IBA for 0.0010 M CPC.	25
7	Plot of Ln (Concentration) vs. Time for 0.0010 M DFP in a Solution of 0.00020 M IBA and 0.0010 M CPC.	26
8	Plot of Ln (Concentration) vs. Time for 0.0010 M DFP in a Solution of 0.00030 M IBA and 0.0010 M CPC.	27
9	Plot of Ln (Concentration) vs. Time for 0.0010 M DFP in a Solution of 0.00040 M IBA and 0.0010 M CPC.	28
10	Plot of Ln (Concentration) vs. Time for 0.0010 M DFP in a Solution of 0.00050 M IBA and 0.0010 M CPC.	29
11	Plot of DFP Hydrolysis Rate Constant vs. CPC Concentration for Five Different Concentrations of IBA (■, 0.00010 M; ▲, 0.00020 M; ◆, 0.00030 M; ●, 0.00040 M; □, 0.00050 M).	32
12	Plot of DFP Hydrolysis Rate Constant vs. IBA Concentration for Six Different Concentrations of CPC (■, 0.0010 M; ▲, 0.0020 M; ◆, 0.0040 M; ●, 0.0070 M; □, 0.0100 M; △, 0.0200 M).	33

List of Tables

<u>Table</u>		<u>Page</u>
I	Apparent Rate Constants for IBA-catalyzed DFP Decomposition at 25°C	31

Analysis by Fourier Transform Infrared Spectrophotometry

Introduction

The college has recently acquired a Nicolet 5DXB Fourier transform infrared (FTIR) spectrophotometer. This instrument has proven to be extremely useful for the evaluation of unusual samples (compared to a typical dispersive infrared spectrophotometer) since the high energy available in the sample compartment allows such techniques as diffuse reflectance (DRIFTS) and attenuated total reflectance (ATR) to be accomplished routinely. Powdered and crystalline materials can, for example, be analyzed for identity in as-received condition, using DRIFTS. Such confirmation of raw material identity is required for all materials that are to be incorporated into a drug product by the federally-mandated Good Manufacturing Practices regulations. ATR is a surface analysis technique that is applicable to smooth, continuous surfaces and has been used in these laboratories to follow the loss of plasticizer from plastic containers at elevated temperature (personal communication with Dr. J.K. Guillory). The circle cell employs a variation of ATR wherein the crystal is formed into a smooth cylinder that resides at the center of the liquid to be analyzed. Using this cell, compounds can be quantitated in aqueous solution.

The use of infrared (IR) spectrophotometry for quantitative purposes was limited at best until the advent of FTIR. Although IR spectrophotometry is inherently less sensitive than ultraviolet (UV) spectrophotometry since vibrational and rotational transitions are being observed as opposed to electronic transitions, the limited quantitative use was mostly a function of the available instrumentation. Infrared sources are hot-wire emitters. While the output from these sources is directly proportional to temperature, the life of the source is inversely related to temperature. The IR energy output that can realistically be obtained from any given source is therefore limited. Further, common IR detectors, whether thermocouple, thermistor, or pyroelectric, have relatively high noise compared to the phototubes used in UV spectrophotometry. In a normal dispersive IR spectrophotometer, the problems of an energy-limited source and a noise-limited detector are made worse by the monochromator and slit system that is required to isolate narrow wavelength regions of the incident radiation.

In an FTIR spectrophotometer, the monochromator/slit system is replaced by a Michelson interferometer. This device allows all wavelengths of radiation to impinge on the sample simultaneously. Absorption of radiation by the sample yields a particular interference pattern or interferogram. This interferogram is the time-domain equivalent of the frequency-domain spectrum that is obtained with a dispersive IR spectrophotometer. Application of the Fourier transform to the interferogram yields the normal frequency-domain spectrum. Additional information on the design and operation of a Michelson interferometer can be found in Griffiths Fourier Transform Infrared Spectrometer (1).

Two important advantages result from the use of an interferometer-based instrument to collect absorption data, these generally being referred to as Jacquinot's Advantage and Fellgett's Advantage. The former states that the throughput of radiation from the source to the detector can be quite high (i.e. efficient) since it is determined solely by the size of the optics. With an interferometric technique, the optics can be quite large since they are not being used to isolate regions of the spectrum. Fellgett's Advantage arises from the fact that each datum point in the interferogram contains a

contribution from every frequency present in the incident radiation. In simplest terms, this means that there will be more information about the interaction between the sample and the incident radiation in an interferogram, and thus the corresponding frequency-domain spectrum, than there is in a spectrum obtained by wavelength isolation. More exactly, the signal-to-noise ratio of a spectrum measured by FTIR spectrophotometry will be greater than the signal-to-noise ratio of a spectrum obtained with a dispersive IR spectrophotometer if the resolution, source, detector, optical throughput and modulation frequency are all equal. This advantage is increased by the ability to co-add successive interferograms prior to performing the Fourier transform. It has been shown that the magnitude of the sample-induced signal increases directly with the number of scans (N) while a truly random noise signal increases in magnitude as the \sqrt{N} . Therefore, co-addition of N scans, with subsequent normalization of the signal level, results in an increase in the signal-to-noise ratio by a factor of \sqrt{N} . These improvements in throughput and signal-to-noise ratio are responsible for making IR spectrophotometry a viable tool for quantitative analysis. This, in conjunction with the specificity afforded by analysis in the IR region, has resulted in the development of specialized attachments, such as those mentioned previously, to handle a wide variety of samples.

It was learned (2) that military usage of topical drug products imposes requirements that are not applicable to typical consumer products. For instance, the preparation must: not cause corrosion or malfunction of equipment that the individual may be expected to use; not increase the visibility of the individual to IR scanning devices; maintain its desired chemical and physical properties over a larger than normal temperature range; be light and compact for ease of carrying; and be easy to apply and remove under field conditions. The requirement of stability over an expanded temperature range is especially troublesome for topical products since such products are usually multiple-phase systems (emulsions and suspensions). It was also learned (2) that the U.S. Army Medical Research and Development Command (USAMRDC) was interested in the various ways that raw material and/or product specifications could be established using FTIR spectrophotometry such that identity, visibility to scanning devices, drug content and so forth could be simultaneously determined. It was agreed that these investigators would both explore such avenues and develop the technical competence of the laboratory workers in the use of this instrument.

Usually, topical preparations are powders, suspensions or emulsions. Both oil-in-water and water-in-oil emulsions are common. To initiate the development of analytical methods employing FTIR spectrophotometry, two projects were devised that had relevance to topical formulations. The first project involved the analysis of the interaction between components of solid formulations that resulted from mechanical processing. The second project involved the quantitative analysis of the internal phase of an emulsion.

Interactions between drugs and dosage form excipients are frequently observed and widely reported in the pharmaceutical literature. The term "interaction" is used here in the broadest sense and may encompass adsorption, complexation, salt formation, or chemical reaction. Such interactions may occur during the manufacture or use of the product and are of obvious concern since they may result in inactivation of the drug. The classical example of this is the interaction of tetracycline and related drugs with divalent and trivalent metal ions in the stomach to form nonabsorbable che-

lates (3-14). While this problem is normally caused by the simultaneous ingestion of drug and either dairy products (4-6,8) or antacids (7,9,13), the same problem can exist if dicalcium phosphate, a common excipient (diluent) in compressed tablets, is incorporated along with tetracycline in the dosage form. Although this latter interaction can obviously occur in the stomach, it can also occur during the manufacturing process if a wet granulation procedure is used.

Interactions between various compounds and polyvinylpyrrolidone have been reported to occur in the solid state (14-24). The analyses of the interaction products were not performed totally in the solid state, however, thus leaving some question about when the reported interactions actually occurred. DRIFTS seemed to be an appropriate way to analyze these claims since the surfaces of the materials in the powdered state could be analyzed directly. These interactions are of interest because they were reported to have occurred as a result of typical manufacturing operations (high speed mixing, grinding, and compression); operations that would be necessary to manufacture a topical powder.

The analysis of water content in pharmaceutical preparations is frequently performed by Karl Fisher titration which is a time-consuming and tedious process. Since water-in-oil emulsions are likely vehicles for the types of barrier formulations discussed (2), it is advantageous to develop more convenient methods for analyzing water content in these systems. It was thought that FTIR spectrophotometry in conjunction with the circle cell attachment might prove to be such a method and this was investigated with a simplified formulation model.

Experimental Methods

One and one-half (1.5) grams of acetaminophen (Sigma Chemical Company, Inc., St. Louis, MO) were gently but thoroughly mixed (no grinding) with 4.5 grams of polyvinylpyrrolidone (approximate molecular weight of 24,000, Aldrich Chemical Company, Inc., Milwaukee, WI) to make 6.0 grams of powder for compression. Five hundred (500) milligrams of this powder (weighed) was placed into a KBr punch and die (Perkin-Elmer Corp., Norwalk, CT) and the assembly was placed between the platens of a hydraulic laboratory press (Pasadena Hydraulics Model P-21, El Monte, CA). Compression pressures were either 87.8, 176, 263, or 351 MPa and compression dwell time was 90 seconds. After the compression process, the tablet was removed from the punch and die and gently broken apart.

Fifty milligrams of each of the previously compressed powders was individually mixed (no grinding) with 250 mg of dry spectral grade KBr (Fisher Scientific, Chicago, IL). These samples were, in turn, transferred to the sample cup of the DRIFTS attachment (Spectra-Tech, Inc., Stamford, CT) and carefully leveled. Samples were scanned 200 times over the 400 cm^{-1} to 600 cm^{-1} range, using a Nicolet 5DXB FTIR (Nicolet Instrument Co., Madison, WI). A resolution of 4 cm^{-1} and a gain of 8 were employed throughout. The sample compartment was continuously purged with dry air and the single beam sample spectra were divided by the single beam spectrum of pure KBr.

Seventeen and one-tenth (17.1) grams of dioctyl sodium sulfosuccinate (Aerosol OT, Fisher Scientific, Chicago, IL) was dissolved in 171 grams of heptane (HPLC grade, Fisher Scientific, Chicago, IL) to make a 10.0% w/w solution. Various quantities (0.0, 0.30, 0.60, 0.90, 1.20, 1.50, 1.80, 2.10, 2.40, 2.70, and 3.00) of double-distilled water were pipetted into 25.0 mL portions of the surfactant in heptane solution and then briefly sonicated. After accounting for the change in volume, the concentrations of water were: 0.0, 1.19, 2.34, 3.47, 4.58, 5.66, 6.72, 7.75, 8.76, 9.75, and 10.71% v/v. Approximately 5 mL of each solution was, in turn, poured into the circle cell (Spectra-Tech, Inc., Stamford, CT) and analyzed. Each infrared absorbance spectrum was obtained with a Nicolet 5DXB FTIR and a dry air purge of the sample compartment was employed. Each spectrum encompassed the 4600 cm^{-1} to 1800 cm^{-1} region and was the result of 200 co-added scans (4 cm^{-1} resolution, gain equal to 4). The single beam sample spectra were divided by the single beam spectrum of the empty cell. The limits for peak integration were 3771.5 cm^{-1} to 3082.4 cm^{-1} .

Results and Discussion

The possibility of manufacturing procedures causing undesired changes in the physical or chemical state of the drug must always be evaluated. Solid state interactions are difficult to verify since most analysis techniques are not applicable to intact powders. If DRIFTS could be successfully used for such purposes, it would simplify the quality control procedures for topical powders. Acetaminophen and polyvinylpyrrolidone were selected because literature precedent indicated that interaction in the solid state was likely.

Compression of a 1:3, weight ratio, mixture of acetaminophen and polyvinylpyrrolidone resulted in a new peak at 1610 cm^{-1} and an enhanced peak at 1561 cm^{-1} compared to the uncompressed physical mixture (Figure 1). Neither of the reactants' spectra showed these features, as demonstrated in Figure 2. Spectra obtained by mathematically adding the individual spectra (both uncompressed material and single component compressed material) resemble the spectrum of the physical mixture as opposed to that of the compressed mixture. Some early success was obtained in correlating the area under the 1610 cm^{-1} peak to compression pressure but the relationship proved impossible to duplicate. When high compression pressures were used, acetaminophen alone also yielded a small peak at 1610 cm^{-1} . Since the area under this peak was substantially smaller than that for the compressed mixture at the same pressure, it was thought that this peak was an artifact resulting from the well-known dependence of DRIFTS on particle size and shape (25-29). It is possible, of course, that the peak at 1610 cm^{-1} that occurred when the physically mixed components were compressed was also an artifact resulting from changes in particle morphology upon compression. The appearance of this peak at lower compression pressure and the larger size of the peak tended to indicate that some surface interaction did occur in the solid state between acetaminophen and polyvinylpyrrolidone. This conclusion cannot be definitively proven at this time.

The dependence of DRIFTS upon particle size and shape (25-29) is not surprising. In normal transmission spectroscopy, distortions in relative band intensities occur if samples are not uniform in thickness and reasonably homogeneous (25). Assuming that the DRIFTS sample cup is reproducibly

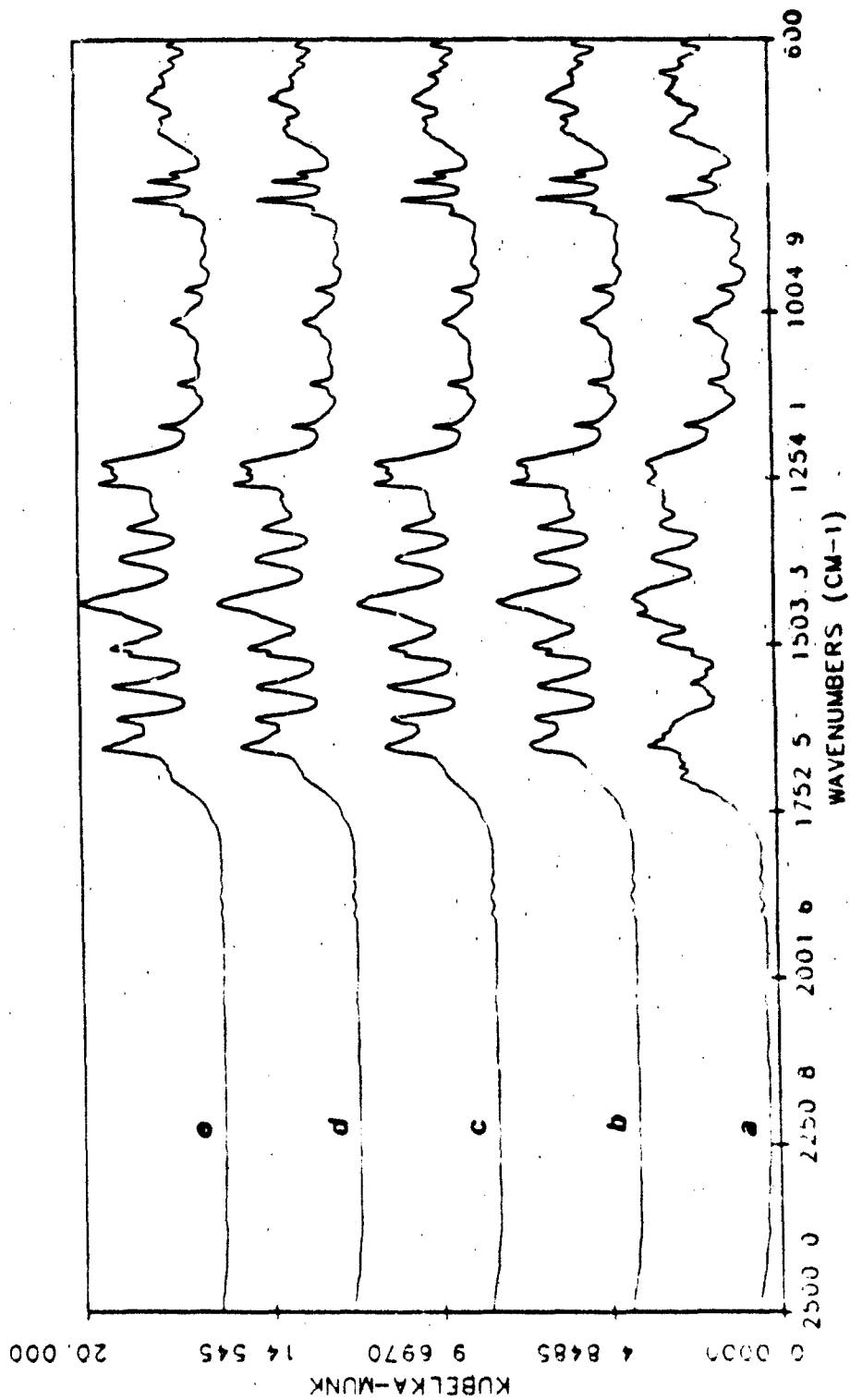


Figure 1. Diffuse Reflectance FTIR Spectra of PVP/APAP Mixtures (3:1 by Weight) at Higher Compression Pressures. a) 0 MPa, b) 67.79 MPa, c) 175.6 MPa, d) 263.4 MPa, e) 351.2 MPa

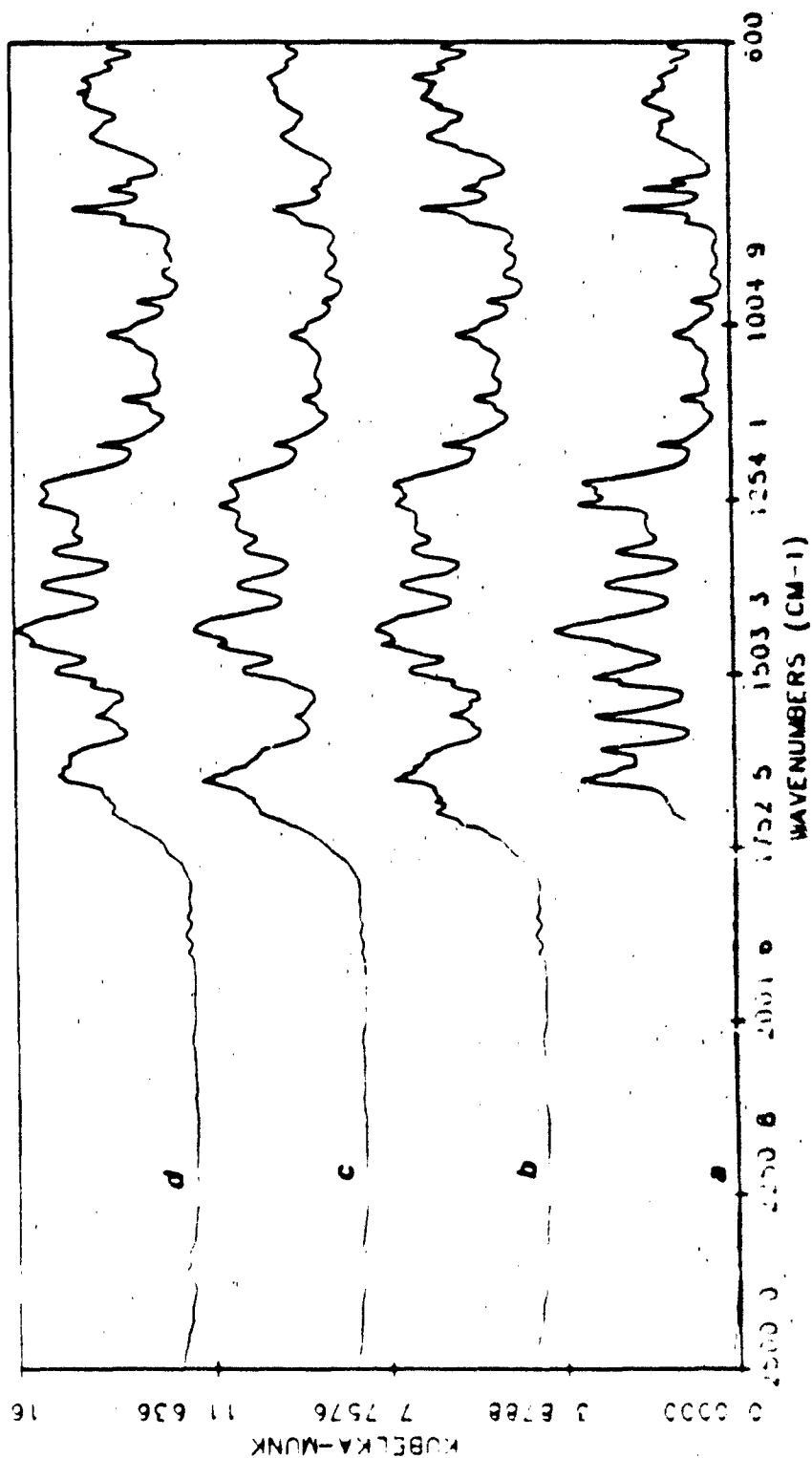


Figure 2. Diffuse Reflectance FTIR Spectra of PVP/APAP Mixtures Compressed, Uncompressed, With and Without Mathematical Spectra Addition. a) PVP/APAP 351.2 MPa compression pressure, b) PVP/APAP physical mixture, c) Mathematical addition of PVP and APAP 351.2 MPa compression pressure in 3:1 ratio, d) Mathematical addition of PVP and APAP 0 MPa compression pressure in 3:1 ratio.

filled, the effective pathlength is related to the path that the incident radiation takes through the powder bed (26). Particle size and shape may have a further effect in that the collection efficiency of the reflected radiation may change (26). Finally, it is necessary to distinguish between diffuse reflectance and specular reflectance. Diffuse reflectance refers to the reflection of radiation that has penetrated some distance into the solid particle before being reflected. The intensities of the various wavelengths of radiation are therefore different in the reflected radiation as a result of the various absorbances of the sample material. Specular reflectance refers to radiation which has been reflected from the particle surface without entering the surface. This reflected radiation is not greatly changed from the incident radiation. Although DRIFTS attachments are designed to minimize the specular component, specular reflectance remains a source of spectrum distortion if the sample absorbance is too high (26,27).

Although it has not been a problem to date, the dependence of DRIFTS on particle size and morphology can be expected to pose problems even when performing single-component quality control (identity) screens on incoming raw materials if those materials are subject to batch-to-batch differences in particle morphology. A common example of this is starch. As a possible solution to this problem, the use of a photoacoustic cell for the FTIR is being investigated. Photoacoustic spectra exhibit changes in overall intensity with surface area, but the changes in relative band intensity frequently seen in DRIFTS spectra with changes in particle diameter and shape seem to occur to a much lesser extent (28,29).

In the circle cell attachment, the liquid to be evaluated engulfs a centrally-located internal reflectance element, usually a zinc selenide crystal. The radiation incident on this crystal establishes a standing wave at the surface which penetrates the test liquid to a depth of approximately 0.1λ , depending upon the actual liquid and crystal used (30). It is this limited depth of radiation penetration that allows solute spectra to be obtained in strongly absorbing solvents.

The determination of the amount of water solubilized in heptane by reverse micelles of dioctyl sodium sulfosuccinate was very successful. Calibration plots of absorption peak area vs. concentration (a typical plot is shown in Figure 3) were quite linear. The correlation coefficients were greater than 0.99 in all cases. It appears from these plots that the method would be useful down to approximately 0.25% v/v water, although standards of this concentration were not prepared. The use of this technique to quantitate water in w/o emulsions of potential use in the formulation of barrier creams is being explored.

A change in priority resulted in the suspension of this work.

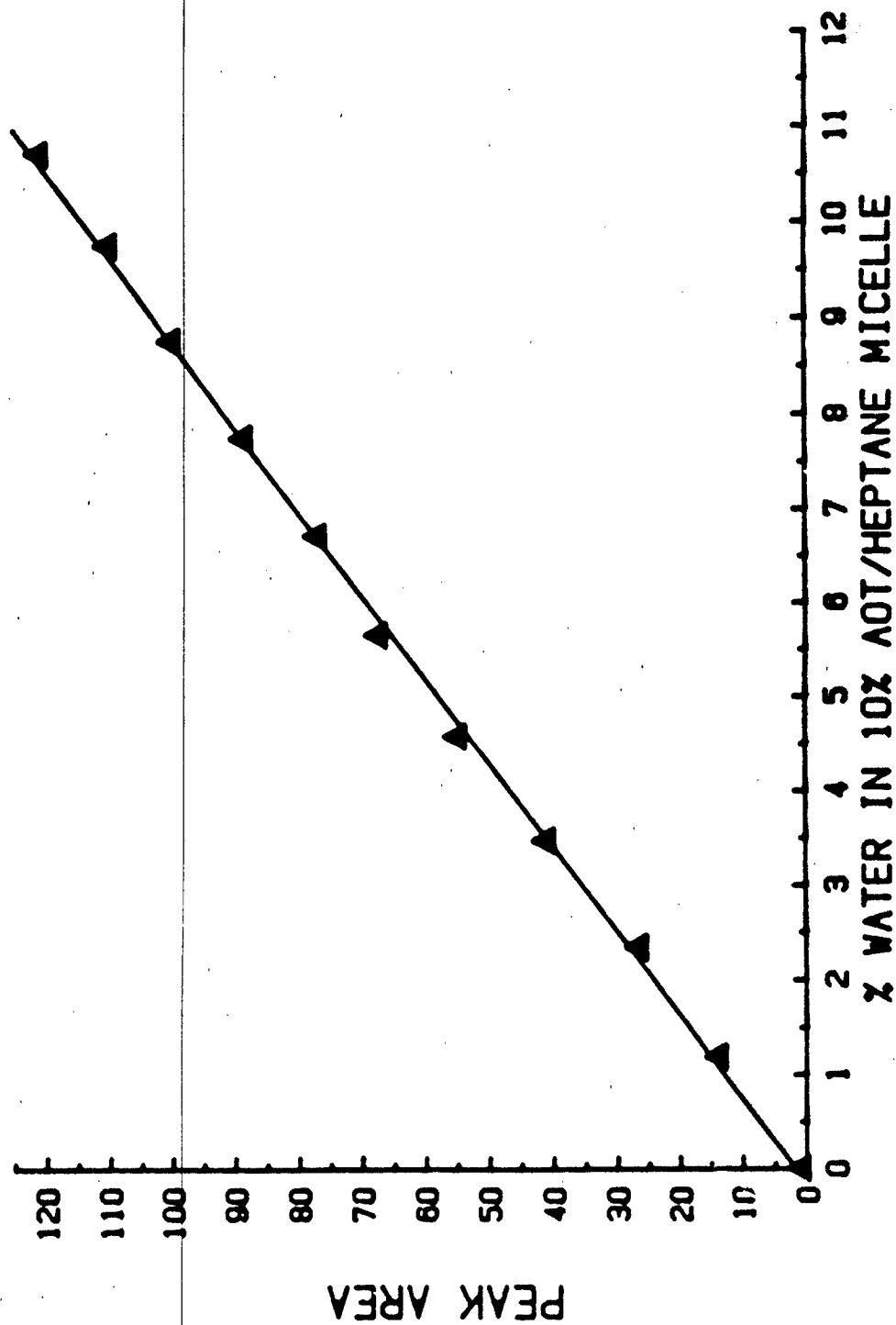


Figure 3. Calibration Plot for Water Solubilized in Heptane by Aerosol OT
(Correlation Coefficient=0.9995).

o-Iodosobenzoic Acid Catalysis

Introduction

Exposure to chemical threat agents can occur in many ways. Direct exposure in a battle situation is obvious. Exposure can also occur indirectly, as in a mechanic working on an airplane or tank that has returned from the battle area. While protection against direct exposure is best accomplished by appropriate apparel, such apparel is not always realistic for personnel operating in a secondary exposure type of environment. In such cases, it would be desirable to have a topical formulation which would protect against skin exposure for a reasonable period of time and then be readily removed (2).

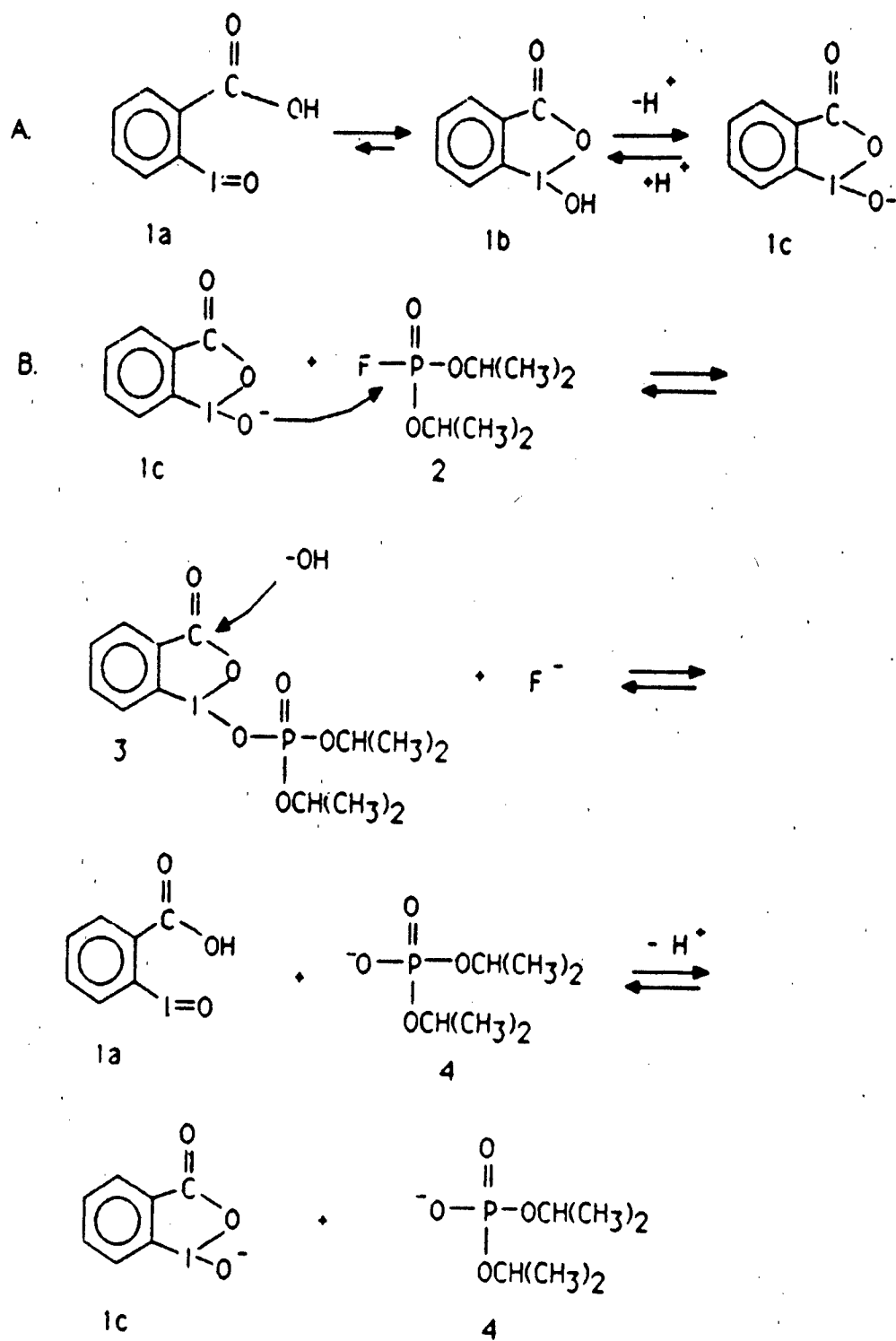
The o-iodosobenzoic acid (IBA) - catalyzed decomposition of esters and phosphonates in micellar media is of interest to USAMRICD because many ester and phosphonate hydrolysis rates can be greatly increased (31-35). Included in the list of compounds for which such acceleration in decomposition has been observed are the chemical threat agents sarin, soman and tabun (31,32). Preliminary attempts at formulating a micellar preparation containing IBA that was suitable for topical application were not successful. In all cases, severe dermal irritation was observed using the rabbit model (2). Presumably this irritation occurred as a result of the cationic surfactants thought to be necessary for IBA activity. It was decided that the investigators at Iowa should assist in this project and that the initial experiments should concentrate on surfactants and model phosphonates for which hydrolysis rate information was available. Work would subsequently center on finding other surfactant or physical systems that would show equal or greater catalytic activity, but, when formulated into topical dosage forms, would have lesser dermal toxicity.

As illustrated by structures 1a and 1b in Figure 4, part A, IBA is tautomeric. It has been found that structure 1b is the predominate form in aqueous solution, a finding which is substantiated by the abnormally high pK_a (~7) reported for this benzoic acid derivative (33,34). Deprotonation of structure 1b gives a nucleophilic I-O anion (structure 1c) at approximately neutral pH.

Figure 4, part B, shows the accepted reaction scheme (33) for IBA and diisopropyl fluorophosphate (DFP), the model compound selected for this work. The nucleophilic attack on DFP by IBA is assumed to be the rate-limiting step. A subsequent nucleophilic attack by hydroxide ion on the IBA-phosphate intermediate generates the 1a form of IBA. Loss of a proton by reestablishment of the expected acid-base equilibrium of IBA regenerates the original nucleophile (structure 1c). This reaction scheme indicates that IBA behaves as a true catalyst, an assumption which has been experimentally verified for DFP (31,32) as well as many other compounds (31-35).

The catalytic activity of IBA has only been observed in systems containing cationic surfactants (31,33-35) or in systems in which the hydroxide counterions on quaternary ammonium derivatized hydrophobic polymeric resins were exchanged for IBA (32, exact resin unspecified). Presumably the polar-nonpolar interface provided by such systems allows both IBA and the substrate to be present in higher concentrations than in the aqueous bulk (33). Although this view is commonly espoused, it has not been proven.

Figure 4. Reaction Scheme for IBA.



Experimental Methods

Various concentrations (0.0010, 0.0020, 0.0040, 0.0070, 0.0100, and 0.0200 M) of cetylpyridinium chloride (CPC, Sigma Chemical Co., Inc., St. Louis, MO) were prepared as 1822 mL batches in 0.055 M phosphate buffer (pH = 7.50). Solutions (0.00010, 0.00020, 0.00030, 0.00040, and 0.00050 M) of IBA (Sigma Chemical Co., Inc., St. Louis, MO) were made using the above surfactant solutions. All five IBA concentrations were employed for each surfactant concentration. Two hundred (200) milliliters of the desired solution was then placed in a polypropylene flask. This flask was put in a water-jacketed glass beaker in order to maintain the solution temperature at $25.0 \pm 0.2^\circ\text{C}$ and the contents of the flask were magnetically stirred. When thermal equilibrium had been achieved, a quantity (35 μL) of DFP (Sigma Chemical Co., Inc., St. Louis, MO) sufficient to make a 0.0010 M solution was added by syringe and concentration measurements were immediately initiated.

DFP hydrolysis was followed by determining the quantity of free fluoride ion appearing in solution as a function of time. This determination was made with an Orion Model 96-09-00 (Orion Research, Inc., Cambridge, MA) fluoride ion electrode (which was left in the test solution throughout the run) and a Corning Model 150 pH/mV meter (Corning Medical and Scientific Instruments, Medford, MA). Fluoride ion calibration curves were prepared by dissolving various amounts of sodium fluoride (Fisher Scientific, Chicago, IL) in pH 7.50 phosphate buffer to make solutions that were 0.0000100 to 0.00100 M in fluoride ion. The solution that was 0.00100 M in free fluoride ion was set to 0.0 mV and the potentials of the other solution concentrations were measured relative to this value.

Results and Discussion

A typical fluoride ion calibration plot is shown in Figure 5. This plot demonstrates the excellent linearity (correlation coefficient=0.9997) obtained with this system over two orders of magnitude of fluoride ion concentration.

To this point the work has only involved one surfactant (CPC) and one test compound (DFP), but a substantial number of conditions have been investigated. Plots of $\ln(\text{DFP})$ vs. time were generally linear through two and one-half half-lives (example plots are shown in Figures 6-10). Occasionally, nonlinear behavior was observed after as little as one half-life. This premature nonlinearity did not seem to correlate with either CPC or IBA concentration and its cause is unknown at this time. The fluoride ion electrode used in the analysis is stated to be nonresponsive to chloride ion. The electrode does respond to hydroxide ion, but the same buffer solution was used to dissolve the NaF for the calibration standards as that used for sample preparation. In the interest of quickly evaluating as many sets of experimental conditions as possible, the NaF standard solutions were prepared without CPC. Since fluoride ion can function as a counterion for the surfactant and since the electrode responds only to free fluoride ion, it is possible that this behavior is responsible for the occasionally observed nonlinearity. Although this is currently being checked, it seems reasonable to assume that all plots would have exhibited deviation from linearity if this phenomenon had been responsible. It may well be that this problem is an experimental artifact and not a systematic error.

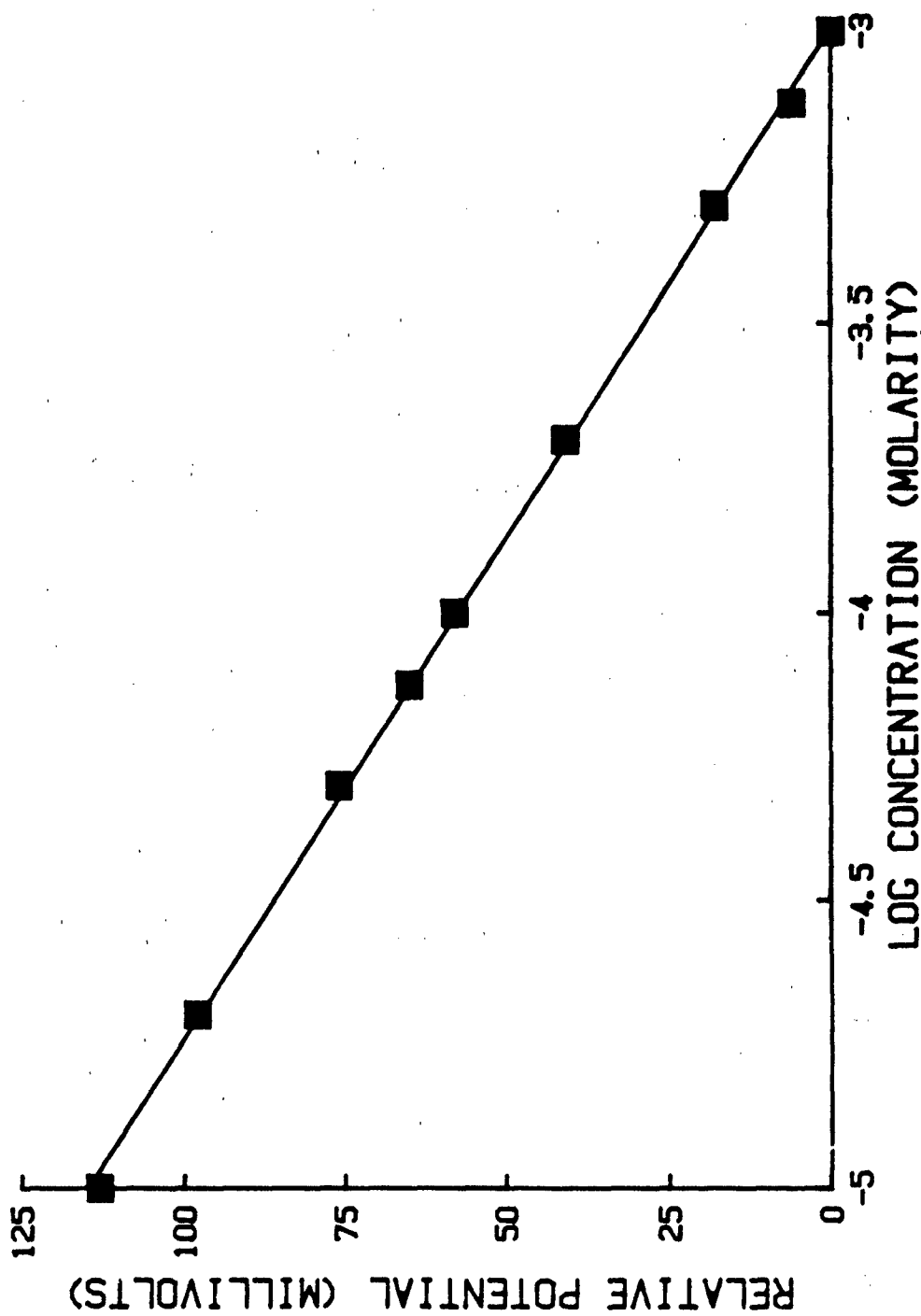


Figure 5. Calibration Plot for the Fluoride Ion Electrode (Correlation

Coefficient=0.9997).

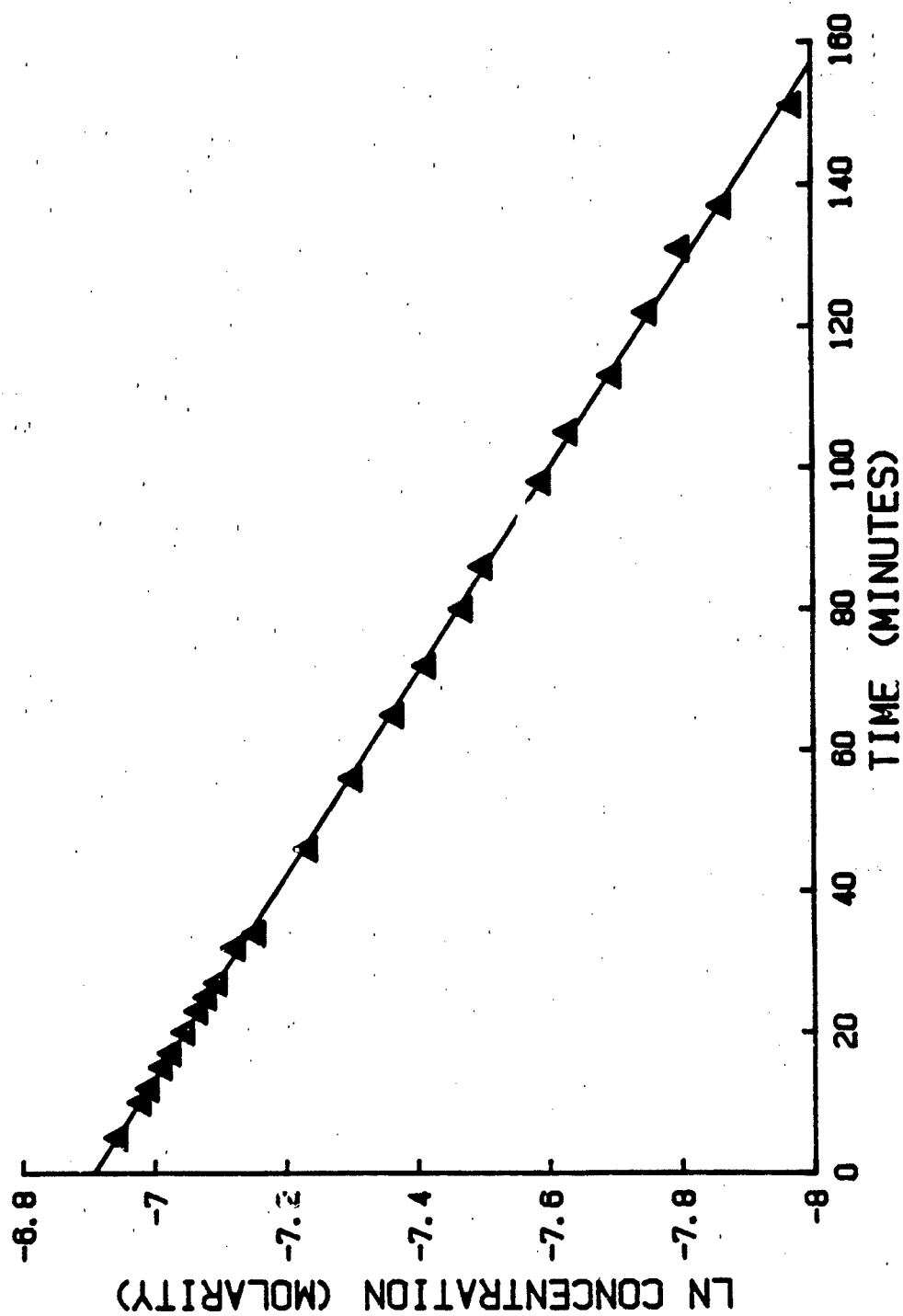


Figure 6. Plot of \ln (Concentration) vs. Time for 0.0010 M DFP in a Solution of 0.00010 M IBA and 0.0010 M CPC.

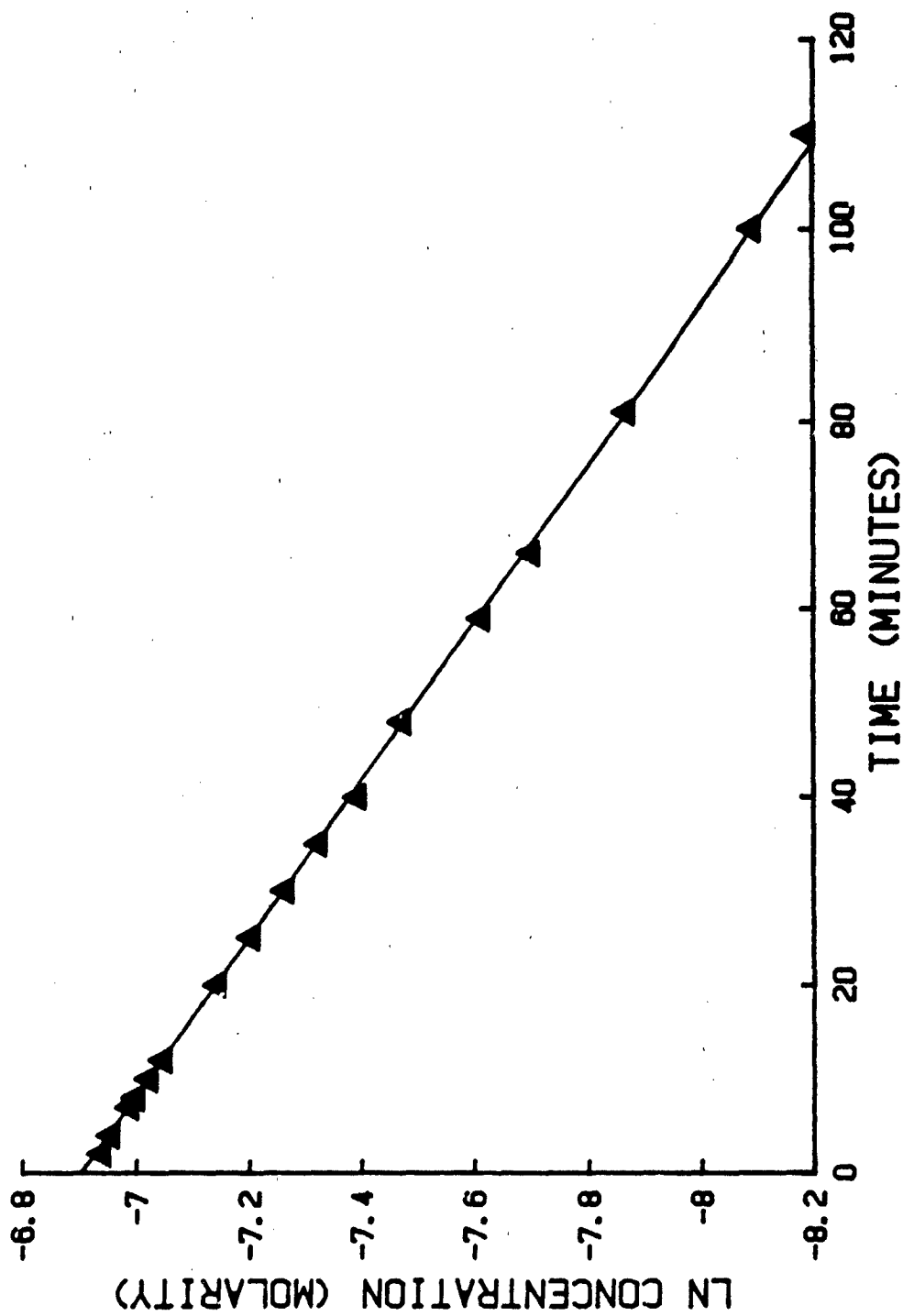


Figure 7. Plot of \ln (Concentration) vs. Time for 0.0010 M DFP in a Solution of 0.00020 M IBA and 0.0010 M CPC.

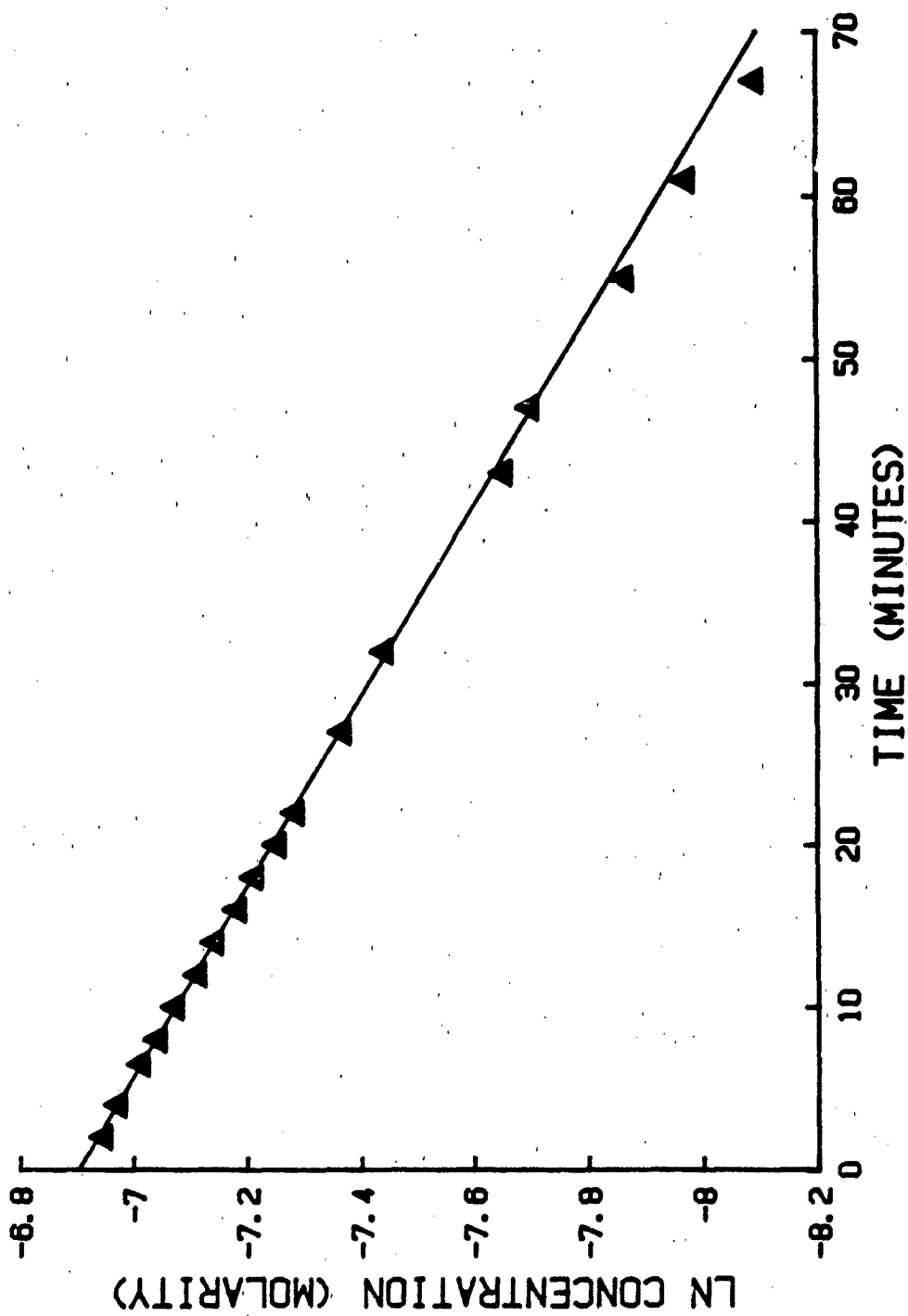


Figure 8. Plot of \ln (Concentration) vs. Time for 0.0010 M DFP in a Solution of 0.00030 M IBA and 0.0010 M CPC.

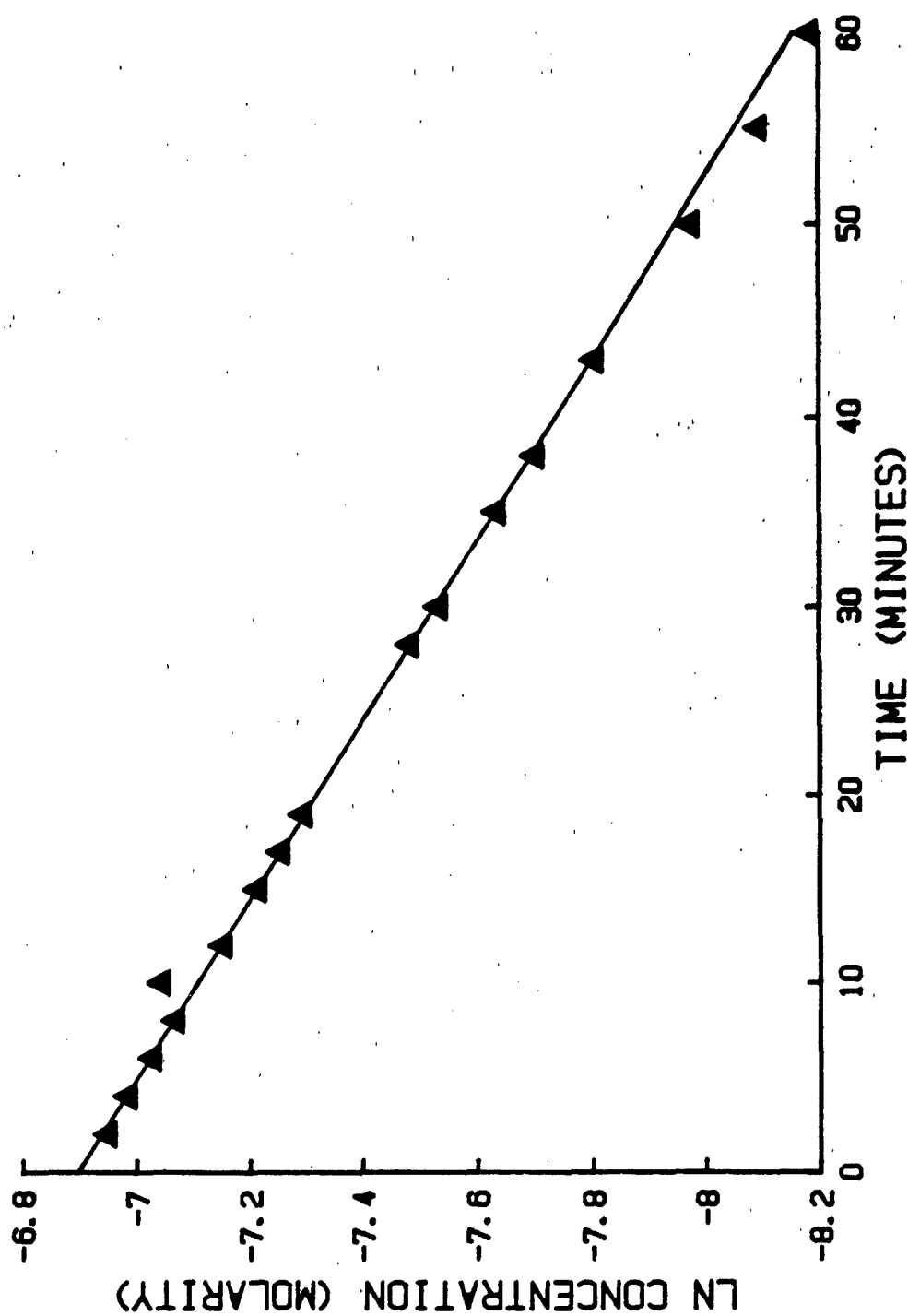


Figure 9. Plot of \ln (Concentration) vs. Time for 0.0010 M DFP in a Solution of 0.00040 M IBA and 0.0010 M GPC.

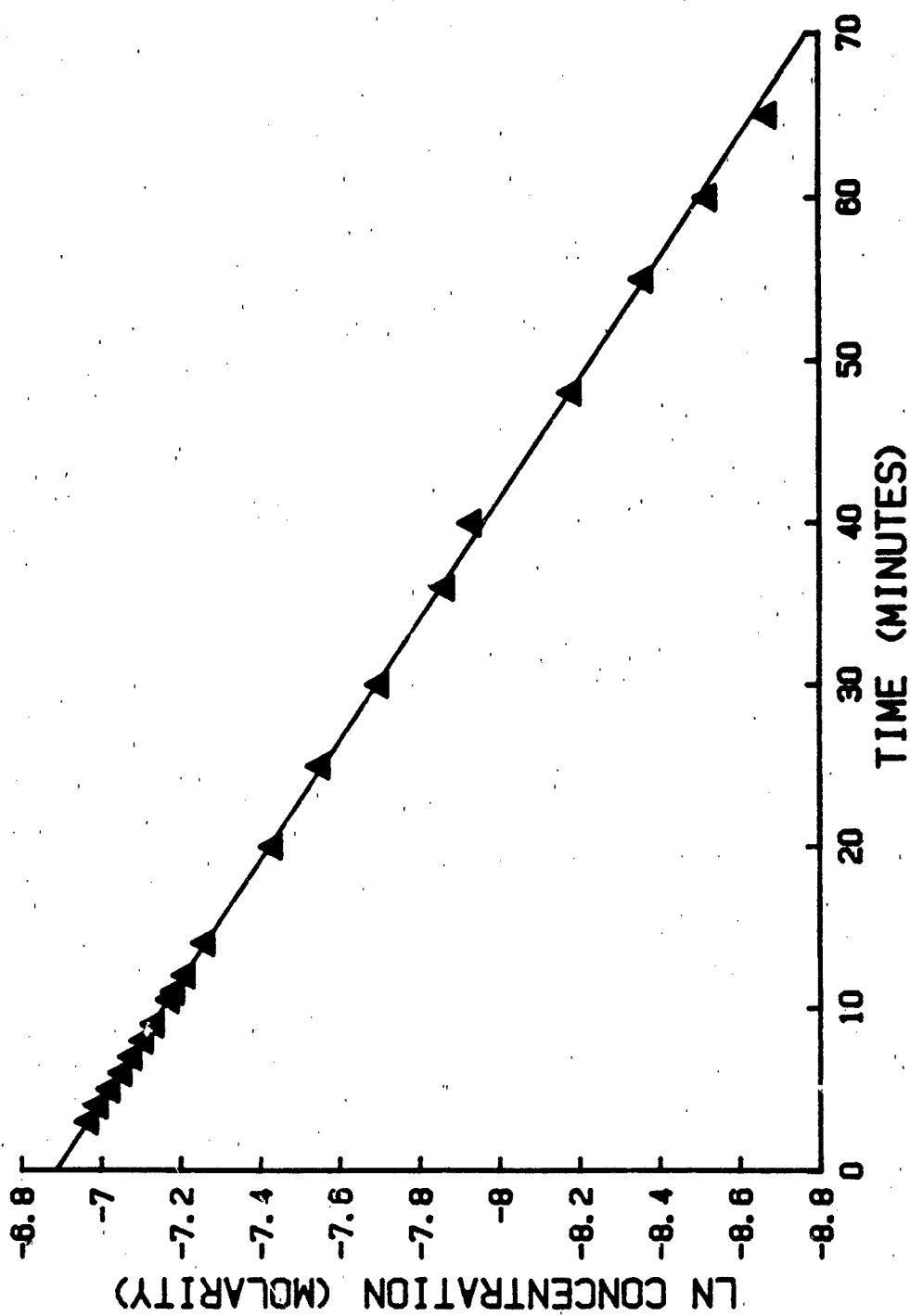


Figure 10. Plot of \ln (Concentration) vs. Time for 0.0010 M DFP in a Solution of 0.00050 M IBA and 0.0010 M CPC.

If the nucleophilic attack of IBA on DFP is the rate-limiting step in the hydrolysis of DFP, then the hydrolysis would be expected to follow second-order kinetics and would be described by the relationship:

$$-\frac{d[\text{DFP}]}{dt} = k[\text{IBA}][\text{DFP}] \quad (1)$$

where the brackets indicate concentration, t is time, and k is the second-order rate constant. Since IBA behaves as a true catalyst, the concentration of IBA does not change during the course of the reaction and equation 1 can be rewritten:

$$-\frac{d[\text{DFP}]}{dt} = k_{\text{app}} [\text{DFP}] \quad (2)$$

where k_{app} is equal to the product of the second-order rate constant and the IBA concentration. It can be seen from equation 2 that the decomposition of DFP should now follow first-order kinetics and the reaction is referred to as being pseudo first-order. The integrated form of equation 2 is:

$$\text{Ln}[\text{DFP}] = \text{Ln}[\text{DFP}]_0 - k_{\text{app}} t \quad (3)$$

where $[\text{DFP}]_0$ is the concentration of DFP at time equal to zero. Equation 3 indicates that a plot of $\text{Ln}[\text{DFP}]$ vs. time should yield a straight line and the obtainment of a straight line through at least two half-life periods provides verification of the reaction order. It can also be seen from equation 3 that the slope of the straight line obtained is equal to $-k_{\text{app}}$.

Since plots of $\text{Ln}[\text{DFP}]$ vs. time were generally linear through at least two and one-half half-lives, a straight line was fit to the linear portion of each plot by least-squares regression analysis and the apparent rate constant for hydrolysis was obtained from the slope of the fitted line. The rate constants so obtained are listed in Table I. The rate constant for decomposition of DFP at 25°C in pH 7.50 phosphate buffer containing 0.0200 M CPC and no IBA was $3.00 \times 10^{-3} \text{ min}^{-1}$ (half-life equal to 231 min.). A plot of k_{app} vs. $[\text{CPC}]$ for five different IBA concentrations demonstrates the expected behavior (Figure 11) for this type of system. The rate constants for DFP decomposition can be seen to increase as a function of total micellar surface area for all IBA concentrations. It appears that this effect reaches a plateau in the vicinity of a 0.01 M CPC concentration. A plateau in reaction rate constant beginning at a surfactant concentration of about 0.01 M was also observed (31,32) for cetyltrimethylammonium chloride (CTAC). Since the latter studies used different substrates, this agreement is probably fortuitous. It would be expected that the position of the plateau would depend upon the molar volume of the substrate, the three-dimensional structure of the substrate as it affected packing in the micelle, and the actual concentration of substrate used.

In Figure 12 the apparent rate constant for DFP hydrolysis is plotted as a function of IBA concentration for six different CPC concentrations. For CPC concentrations of 0.0070 M or less, the hydrolysis rate constant increases linearly as a function of IBA concentration (correlation coefficient=0.997). This behavior has also been observed (33) for the IBA-catalyzed decomposition of 4-nitrophenyl diphenyl phosphate in a cetyltrimethylammonium bromide microemulsion. The data for CPC concentrations of 0.0100 and 0.0200 M are confusing. At a concentration of 0.0100 M CPC, the data appear to be approaching a plateau in a first-order manner. The data

Table I
Apparent Rate Constants for IBA-catalyzed DFP Decomposition at 25°C

Surfactant Concentration (Molarity)	IBA Concentration (Molarity)	Rate Constant (Min ⁻¹)	Half-Life (Min ⁻¹)
0.0010	1.0 x 10 ⁻⁴	6.96 x 10 ⁻³	99.6
	2.0 x 10 ⁻⁴	1.19 x 10 ⁻²	58.3
	3.0 x 10 ⁻⁴	1.70 x 10 ⁻²	40.7
	4.0 x 10 ⁻⁴	2.10 x 10 ⁻²	33.1
	5.0 x 10 ⁻⁴	2.69 x 10 ⁻²	25.8
0.0020	1.0 x 10 ⁻⁴	8.22 x 10 ⁻³	84.3
	2.0 x 10 ⁻⁴	1.25 x 10 ⁻²	55.3
	3.0 x 10 ⁻⁴	1.96 x 10 ⁻²	35.4
	4.0 x 10 ⁻⁴	2.54 x 10 ⁻²	27.3
	5.0 x 10 ⁻⁴	3.13 x 10 ⁻²	22.2
0.0040	1.0 x 10 ⁻⁴	1.09 x 10 ⁻²	63.7
	2.0 x 10 ⁻⁴	1.94 x 10 ⁻²	35.8
	3.0 x 10 ⁻⁴	2.65 x 10 ⁻²	26.1
	4.0 x 10 ⁻⁴	3.41 x 10 ⁻²	20.3
	5.0 x 10 ⁻⁴	4.47 x 10 ⁻²	15.5
0.0070	1.0 x 10 ⁻⁴	1.37 x 10 ⁻²	50.7
	2.0 x 10 ⁻⁴	3.55 x 10 ⁻²	27.1
	3.0 x 10 ⁻⁴	3.61 x 10 ⁻²	19.2
	4.0 x 10 ⁻⁴	4.66 x 10 ⁻²	14.9
	5.0 x 10 ⁻⁴	5.40 x 10 ⁻²	12.8
0.0100	1.0 x 10 ⁻⁴	2.00 x 10 ⁻²	34.6
	2.0 x 10 ⁻⁴	3.82 x 10 ⁻²	18.1
	3.0 x 10 ⁻⁴	5.74 x 10 ⁻²	12.1
	4.0 x 10 ⁻⁴	6.79 x 10 ⁻²	10.2
	5.0 x 10 ⁻⁴	7.80 x 10 ⁻²	8.9
0.0200	1.0 x 10 ⁻⁴	2.28 x 10 ⁻²	30.4
	2.0 x 10 ⁻⁴	3.11 x 10 ⁻²	22.3
	3.0 x 10 ⁻⁴	6.06 x 10 ⁻²	11.4
	4.0 x 10 ⁻⁴	6.27 x 10 ⁻²	11.0
	5.0 x 10 ⁻⁴	8.30 x 10 ⁻²	8.4

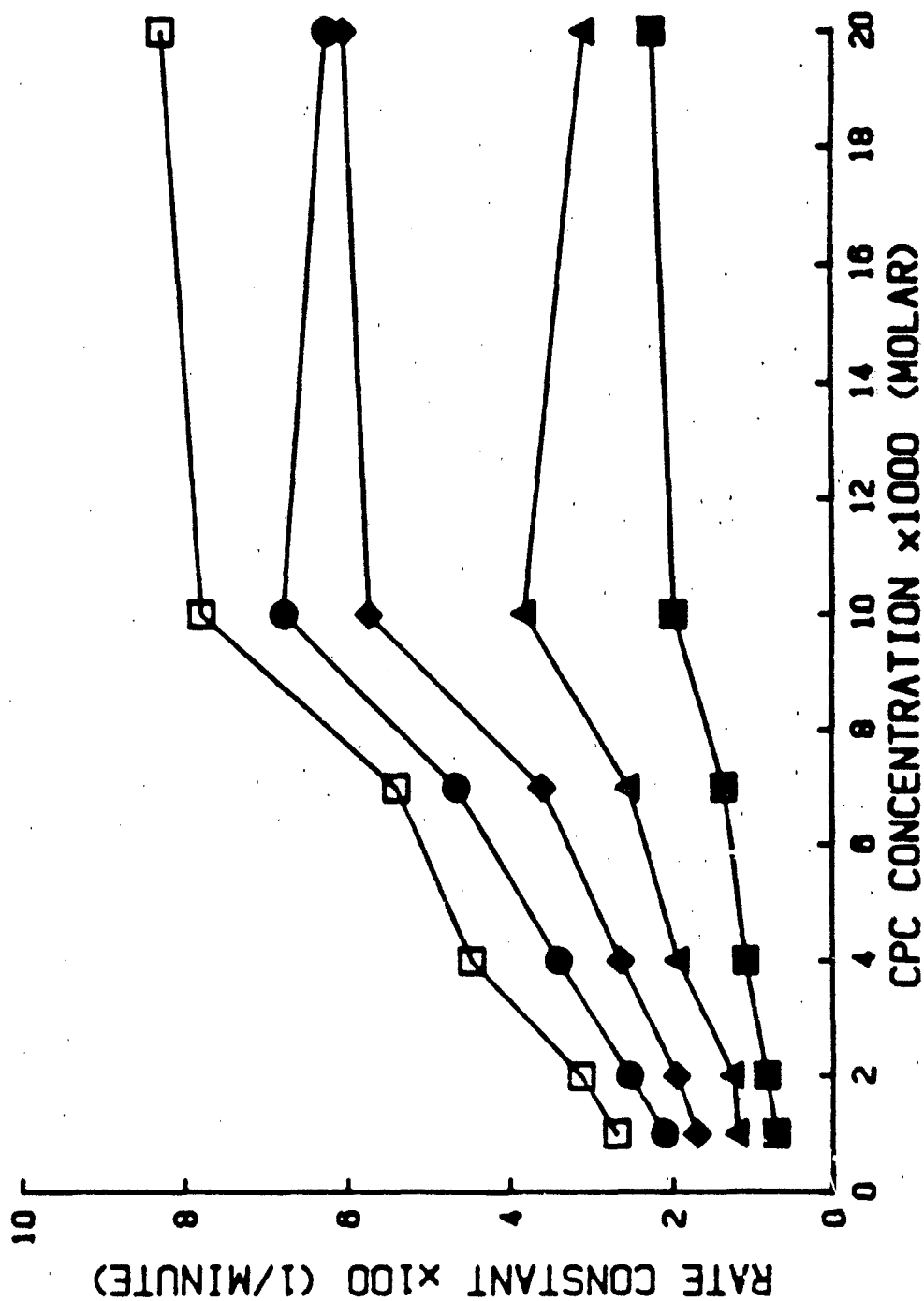


Figure 11. Plot of DFP Hydrolysis Rate Constant vs. CPC Concentration for Five Different Concentrations of IBA (■, 0.00010 M; ▲, 0.00020 M; ◆, 0.00030 M; ●, 0.00040 M; □, 0.00050 M).

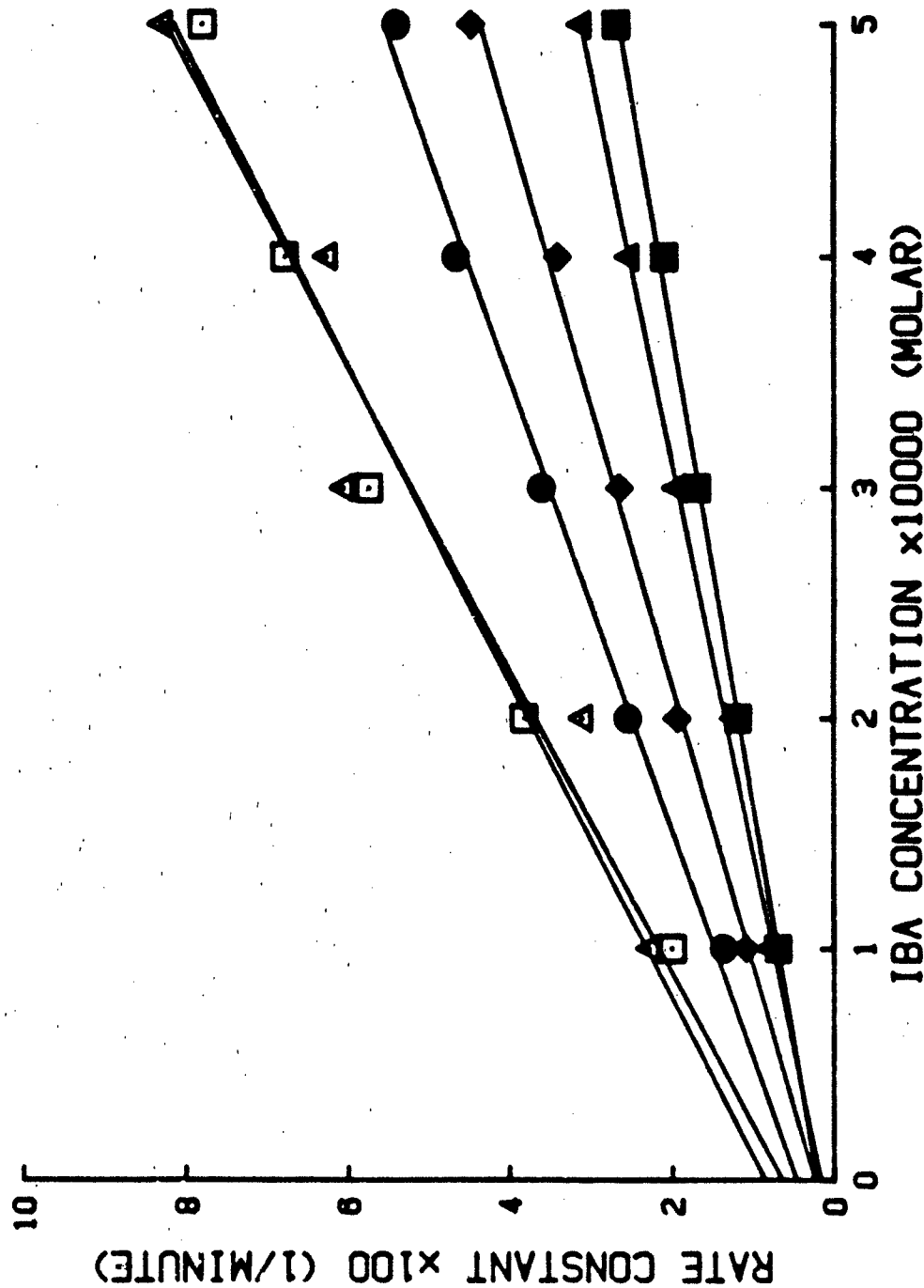


Figure 12. Plot of DFP Hydrolysis Rate Constant vs. IBA Concentration for Six Different Concentrations of CPC (◆, 0.0010 M; ▲, 0.0020 M; ●, 0.0040 M; ●, 0.0070 M; □, 0.0100 M; △, 0.0200 M).

for 0.0200 M CPC once again look linear but with extremely high variability. This may simply be a result of having only one run for each set of experimental conditions. It is also possible that there is an underlying physicochemical reason for this behavior that remains to be characterized.

Durst et al. (31) have reported a range of 715-754 seconds for the hydrolysis half-life of DFP in a micellar system containing 0.00099 M IBA (0.0059-0.0066 M CTAC, 0.00116 M DFP; temperature, buffer, and pH unspecified but assumed to be 25°C, phosphate, and 7.5, respectively). Our closest experimental condition was 0.00050 M IBA, 0.0070 M CPC, 0.0010 M DFP, 25°C, phosphate buffer, and pH=7.50. For this set of conditions, the half-life for DFP hydrolysis was found to be 768 seconds. This result is reasonable in view of the different surfactants employed and the different IBA concentrations.

Current work is directed toward the determination of the effect of CPC addition on the calibration plots for fluoride ion. Subsequently, studies of the accelerated hydrolysis of DFP by IBA will be conducted using cetyltrimethylammonium bromide as the surfactant in place of CPC. At this point, all data collected will be evaluated and certain sets of experimental conditions will be selected for use in determining the effect of pH on the catalysis.

It will also be necessary to start evaluating other surfactants for catalyst system suitability. Although not definitively proven, the cationic surfactants are presumed by these investigators to be responsible for the dermal toxicity observed with trial topical formulations. The obvious approach is to conduct additional kinetic studies determine whether IBA still catalyzes the decomposition of DFP when other surfactant systems are employed. When experiments were carried out with various Tweens, no catalytic activity was observed (36). Presumably, the position of IBA and/or DFP solubilization in the micelle was changed by the absence of the charged head group. It may be possible to restore activity by adsorbing cations from solution onto the micelle surface. If this technique is successful in restoring catalysis, there is some possibility that it might also restore dermal toxicity. All catalytically successful systems will be tested for dermal toxicity using the rabbit model. Proper orientation of IBA and DFP in the micelle might also be restored by using nonionic surfactants with different hydrophile/lipophile balances, by selecting surfactants with different head group diameters, and so forth. Such experimentation will be time consuming, since it appears little is known about the structural requirements for the micelle except that quaternary amine surfactants work. A trial and error approach will be necessary.

Ideally, a successful barrier formulation will be one which: provides ten half-lives of reaction in ten minutes under field conditions, is nontoxic to the skin, can be applied easily and quickly, can be readily removed when contaminated, interferes minimally with the normal physiology of the skin, does not cause corrosion or improper operation of necessary field equipment, and is chemically and physically stable over a wide range of temperature. In total, these are difficult requirements to meet and some compromise may be necessary. These requirements will, however, serve as a means of selecting the best possible formulation.

Conclusions

Although a change in priority has resulted in the suspension of FTIR spectrophotometry methods development, it is believed that the demonstrated ability to analyze water in water-in-oil emulsions will be quite useful in the future.

As expected, the IBA-catalyzed decomposition of DFP in micellar media was found to follow pseudo first-order kinetics. Both the concentration of the cationic surfactant and the concentration of IBA were found to influence DFP decomposition rate. A twelve-fold decrease in DFP half-life was observed when a solution that was 0.0200 M in CPC and 0.00050 M in IBA was compared to a solution that was 0.0010 M in CPC and 0.00010 M in IBA. Since catalytic activity is lost when nonionic surfactants are employed (36) and since the cationic surfactants used in this work frequently cause dermal irritation, successful use of IBA in topical protectant formulations will require that the exact structural requirements for the micelle be determined.

References

1. Griffiths, P.R. and de Haseth, J.A., Fourier Transform Infrared Spectrometry, John Wiley and Sons, Inc., New York, NY, 1986, pp. 1-80.
2. Personal Communication with LTC Reardon of USAMRICD.
3. Penttila, O., and others, Eur. J. Clin. Pharmacol., "Effect of Zinc Sulphate on the Absorption of Tetracycline and Doxycycline in Man," 9, 31 (1975).
4. Scheiner, J., and Altemeier, W.A., Surg. Gynecol. Obstet., "Experimental Study of Factors Inhibiting Absorption and Effective Therapeutic Levels of Declomycin," 114, 9 (1962).
5. Rosenblatt, J.E., and others, Antimicrob. Agents Chemother., "Comparison of in vitro Activity and Clinical Pharmacology of Doxycycline with other Tetracyclines," 6, 134 (1966).
6. Mattila, M.J. and others, Excerpta Medica Int. Cong. Ser., "Interference of Iron Preparations and Milk with the Absorption of Tetracyclines," 254, 128 (1971).
7. Waisbren, B.A., and Hueckel, J.S., Proc. Soc. Exp. Biol. Med., "Reduced Absorption of Aureomycin Caused by Aluminum Hydroxide Gel (Amphojel)," 73, 73 (1950).
8. Boger, W.P., and Gavin, J.J., N. Engl. J. Med., "An Evaluation of Tetracycline Preparations," 261, 827 (1959).
9. Garty, M., and Hurwitz, A., Clin. Pharmacol. Ther., "Effect of Cimetidine and Antacids on Gastrointestinal Absorption of Tetracycline," 28, 203 (1980).
10. Albert, K.A., and others, J. Pharm. Sci., "Decreased Tetracycline Bioavailability Caused by a Bismuth Subsalicylate Antidiarrheal Mixture," 68, 586 (1979).
11. Ericsson, C.D., and others, J.A.M.A., "Influence of Subsalicylate Bismuth on Absorption of Doxycycline," 247, 2266 (1982).
12. Albert, A., and Rees, C.W., Nature, "Avidity of the Tetracyclines for the Cations of Metals," 177, 443 (1956).
13. Chin, T.F., and Lach, J.L., Am. J. Hosp. Pharm., "Drug Diffusion and Bioavailability: Tetracycline Metallic Chelation," 32, 625 (1975).
14. Jürgensen-Eide, G.J., and Speiser, P., Acta Pharmaceutica Suecica, "Interaction Between Drugs and Nonionic Macromolecules. I," 4, 185 (1967).
15. Jürgensen-Eide, G.J., and Speiser, P., Acta Pharmaceutica Suecica, "Interaction Between Drugs and Nonionic Macromolecules. II," 4, 201 (1967).

16. Frömming, K.H., Ditter, W., and Horn, D., *Journal of Pharmaceutical Sciences*, "Sorption Properties of Cross-linked Insoluble polyvinylpyrrolidone," 70, 738 (1981).
17. Plaizier-Vercammen, J.A., and DeNève, R.E., *Journal of Pharmaceutical Sciences*, "Interaction of Povidone with Aromatic Compounds. III. Thermodynamics of Binding and Interaction Forces in Buffer Solutions of Varying pH Value and Dielectric Constant," 71, 552 (1982).
18. Thoma, V.K., and Steinbach, D., *Pharmaceutische Industrie*, "Untersuchungen über das Bindungsvermögen von Polyvinylpyrrolidon für Bisazofarbstoffe," 38, 841 (1976).
19. Kahela, P., and Krogerus, V.E., *Farmaseuttinen Aikakauslehti*, "On the Rate of Release of Active Ingredient from the Polyvinylpyrrolidone (PVP) Tablets. I. The Release of Benzoic Acid and o-, m-, and p-Hydroxybenzoic Acids," 79, 74 (1970).
20. Kahela, P., and Krogerus, V.E., *Farmaseuttinen Aikakauslehti*, "On the Rate of Release of Active Ingredient from the Polyvinylpyrrolidone (PVP) Tablets. II. The Release of Dihydroxybenzoic Acids and Gallic Acid," 79, 117 (1970).
21. Kahela, P., and Krogerus, V.E., *Farmaseuttinen Aikakauslehti*, "On the Rate of Release of Active Ingredient from the Polyvinylpyrrolidone (PVP) Tablets. III. The Release of p-Aminobenzoic Acid and Salicylic Acid Amide Compared with Benzoic Acid, Salicylic Acid and p-Hydroxybenzoic Acid," 79, 148 (1970).
22. Kahela, P., and Krogerus, V.E., *Farmaseuttinen Aikakauslehti*, "Nuclear Magnetic Resonance and Infrared Spectroscopic Study of the Interaction of Polyvinylpyrrolidone (PVP) with Benzoic Acid and Salicylic Acid," 80, 220 (1971).
23. Kahela, P., Perälä-Suominen, A., and Voutilainen, P., *Farmaseuttinen Aikakauslehti*, "On the Effect of Polyvinylpyrrolidone on the Absorption of Benzoic Acid and its Hydroxy Derivatives," 80, 331 (1971).
24. Mayersohn, M., and Gibaldi, M., *Journal of Pharmaceutical Sciences*, "New Method of Solid State Dispersion for Increasing Dissolution Rates," 55, 1323 (1966).
25. Crocombe, R.A., Olson, M.L., and Hill, S.L., "Quantitative Fourier Transform Infrared Methods for Real Complex Samples," Computerized Quantitative Infrared Analysis, ASTM STP 934, G.L. McClure, Ed., American Society for Testing and Materials, Philadelphia, PA, 1987, pp. 95-130.
26. Griffiths, P.R., and de Haseth, J.A., Fourier Transform Infrared Spectrometry, John Wiley and Sons, Inc., New York, NY, 1986, pp. 544-546.
27. Ibid, pp. 197-202.
28. Ibid, p. 332.

29. Childers, J.W., and Palmer, R.A., American Laboratory, "A Comparison of Photoacoustic and Diffuse Reflectance Detection in FTIR Spectrometry," 18, 22 (1986).
30. Griffiths, P.R., and de Haseth, J.A., Fourier Transform Infrared Spectrometry, John Wiley and Sons, Inc., New York, NY, 1986, pp. 193-194.
31. Durst, H.D., Seiders, R., Albizo, J., Hammond, P.S., Forster, J., Farmer, A., Duell, B.L., and Katritzky, A.R., "Hydrolysis of Fluorophosphonates and Other Derivatives," Proceedings of the 1985 Scientific Conference on Chemical Defense Research, April 1986.
32. Hammond, P.S., Forster, J., Farmer, A., and Durst, H.D., "Update on the Use of o-Iodosobenzoic Acid and Its Derivatives for Skin Decontamination/Prophylactin Applications," manuscript copy supplied by P.S. Hammond.
33. Mackay, R.A., Longo, F.R., Knier, B.L., and Durst, H.D., J. Phys. Chem., "Iodosobenzoate Catalyzed Hydrolysis of 4-Hitrophenyl Diphenyl Phosphate in a CTAM Microemulsion," 91, 861-864 (1987).
34. Moss, R.A., Alwis, K.W., and Bizzigotti, G.O., J. Am. Chem. Soc., "o-Iodosbenzoate: Catalyst for the Micellar Cleavage of Activated Esters and Phosphates," 105, 681-682 (1983).
35. Moss, R.A., Alwis, K.W., and Shin, J.-S., J. Am. Chem. Soc., "Catalytic Cleavage of Active Phosphate and Ester Substrates by Iodoso- and Iodoxybenzoates," 106, 2651-2655 (1984).
36. Personal Communication with P. Hammond of USAMRICD.

DISTRIBUTION LIST

1 Copy Commander
US Army Medical Research and Development Command
ATTN: SGRD-RMI-S
Fort Detrick, Frederick, Maryland 21701-5012

5 copies Commander
US Army Medical Research and Development Command
ATTN: SGRD-PLS
Fort Detrick, Frederick, Maryland 21701-5012

2 copies Defense Technical Information Center (DTIC)
ATTN: DTIC-DDAC
Cameron Station
Alexandria, VA 22304-6145

1 copy Dean
School of Medicine
Uniformed Services University of the
Health Sciences
4301 Jones Bridge Road
Bethesda, MD 20814-4799

1 copy Commandant
Academy of Health Sciences, US Army
ATTN: AHS-CDM
Fort Sam Houston, TX 78234-6100